Monthly Notices
of the
ROYAL ASTRONOMICAL SOCIETY

Mon. Not. R. Astron. Soc. **413,** 1165–1173 (2011) doi:10.1111/j.1365-2966.2011.18209.x

# Redshifted H I and OH absorption in radio galaxies and quasars

S. J. Curran,[1⋆] M. T. Whiting,[1,2] M. T. Murphy,[3,4] J. K. Webb,[1] C. Bignell,[5] A. G. Polatidis,[6,7] T. Wiklind,[8,9,10] P. Francis[11] and G. Langston[5]

[1]*School of Physics, University of New South Wales, Sydney, NSW 2052, Australia*
[2]*CSIRO Australia Telescope National Facility, PO Box 76, Epping, NSW 1710, Australia*
[3]*Institute of Astronomy, University of Cambridge, Madingley Road, Cambridge CB3 0HA*
[4]*Centre for Astrophysics and Supercomputing, Swinburne University of Technology, PO Box 218, Hawthorn, VIC 3122, Australia*
[5]*National Radio Astronomy Observatory, PO Box 2, Rt. 28/92 Green Bank, WV 24944-0002, USA*
[6]*Max-Planck-Institut für Radioastronomie, Postfach 2024, D-53010 Bonn, Germany*
[7]*Netherlands Institute for Radio Astronomy (ASTRON), Postbus 2, 7990 AA Dwingeloo, the Netherlands*
[8]*Onsala Space Observatory, S-439 92 Onsala, Sweden*
[9]*Space Telescope Science Institute, 3700 San Martin Drive, Baltimore, MD 21218-2463, USA*
[10]*Joint ALMA Observatory, Santiago, Chile*
[11]*Department of Physics, Australian National University, ACT 0200, Australia*

Accepted 2010 December 14. Received 2010 December 1; in original form 2010 September 3

**ABSTRACT**

From a survey for the redshifted H I 21-cm and OH 18-cm absorption in the hosts of a sample of radio galaxies and quasars, we detect H I in three of the 10 and OH in none of the 14 sources for which useful data were obtained. As expected from our recent result, all of the 21-cm detections occur in sources with ultraviolet (UV) continuum luminosities of $L_{\rm UV} \leq 10^{23}$ W Hz$^{-1}$. At these 'moderate' luminosities, we also obtain four non-detections, although, as confirmed by the equipartition of detections between the type 1 and type 2 objects, this near-50 per cent detection rate cannot be attributed to unified schemes of active galactic nuclei (AGNs). All of our detections are at redshifts of $z \lesssim 0.67$, which, in conjunction with our faint source selection, biases against UV luminous objects. The importance of the UV luminosity (over AGN type) in the detection of the 21-cm absorption is further supported by the non-detections in the two high-redshift ($z \sim 3.6$–$3.8$) radio galaxies, which are both type 2 objects, while having $L_{\rm UV} > 10^{23}$ W Hz$^{-1}$. Our 21-cm detections in combination with those previously published give a total of eight (associated and intervening) H I-absorbing sources searched and undetected in OH. Using the detected 21-cm line strengths to normalize the limits, we find that only two of these eight sources may have been searched sufficiently deeply in OH, even though these are marginal.

**Key words:** galaxies: active – galaxies: fundamental parameters – galaxies: high-redshift – quasars: absorption lines – radio lines: galaxies – ultraviolet: galaxies.

## 1 INTRODUCTION

Although opaque to optical light, the dusty Universe is transparent to radiation at radio wavelengths, thus making the spectroscopic study of the 21-cm spin-flip transition of neutral hydrogen (H I) a very useful tool in probing the far reaches of the cosmos. The low probability of the transition compounded by the inverse square law renders H I 21-cm absorption currently undetectable in emission at redshifts of $z \gtrsim 0.1$. However, in the absorption of radio waves emitted from background quasars, the line strength depends only upon the column density of the absorber and the flux of the background source. Therefore, by using absorption lines, we can, in principle, probe H I to redshifts of $z \sim 50$ (or when the Universe was 1 per cent its present age), where the ionosphere begins to affect low-frequency radio waves ($\lesssim$30 MHz). With such observations we can address several outstanding questions in cosmology and fundamental physics:

(i) Probe the epoch of re-ionization when the first ever stars ignited, re-ionizing the gas in the smaller cosmos (e.g. Carilli et al. 2004).

(ii) Determine the contribution of the neutral gas content to the mass density of the Universe (Kanekar et al. 2009; Curran 2010).

(iii) Measure any putative variations in the values of the fundamental constants of nature at large look-back times, to at least

⋆E-mail: sjc@phys.unsw.edu.au

an order of magnitude of the sensitivity provided by the best optical data (see Tzanavaris et al. 2007). This offers one of the few experimental tests of current Grand Unified Theories, thus having profound implications for modern physics.

The latter point requires the comparison of the redshift of the 21-cm line with other transitions, which may be optical/ultraviolet (UV) [from singly ionized metals, giving $\Delta(\mu\alpha^2 g_{\rm p})/\mu\alpha^2 g_{\rm p}$], where $\alpha$ is the fine structure constant, $\mu$ the electron-to-proton mass ratio and $g_{\rm p}$ the proton $g$-factor, millimetre-wave [rotational transition of molecules, giving $\Delta(\alpha^2 g_{\rm p})/\alpha^2 g_{\rm p}$] or other decimetre transitions (see Curran, Kanekar & Darling 2004a and references therein), specifically, transitions arising from the hydroxyl radical (OH), which can also be intracompared (Darling 2003), thus avoiding possible line-of-sight effects which could mimic a change in the constants.

Thus, highly redshifted H I 21-cm and OH 18-cm absorbers are of great interest, although these are currently very rare, with only 73 H I 21-cm absorption systems at $z \geq 0.1$ known – 41 of which occur in galaxies intervening the sight-lines to more distant quasars (see table 1 of Curran 2010), with the remainder arising in the host galaxies of the quasars themselves (see table 1 of Curran & Whiting 2010). In the case of OH, the situation is more dire with only five absorbers currently known (Chengalur, de Bruyn & Narasimha 1999; Kanekar & Chengalur 2002; Kanekar et al. 2003, 2005). Four of these were originally found through millimetre-wave molecular absorption, although further surveys have proven futile (see Curran et al. 2004b), which we suggest is due to the traditional optical selection of the sources. The target of choice in many previous surveys has been damped Lyman $\alpha$ absorption systems (DLAs), since these are known to contain large columns of neutral hydrogen ($N_{\rm H\,I} \geq 2 \times 10^{20}$ cm$^{-2}$, by definition) at precisely determined redshifts. Although 19 DLAs have been detected in the $H_2$ Lyman and Werner UV bands (see Noterdaeme et al. 2008; Jorgenson et al. 2009; Srianand et al. 2010), these are at molecular fractions well below the detection thresholds of current microwave instruments (Curran et al. 2004b). Furthermore, the molecular abundances appear to be correlated with the colour of the background quasar in that the DLAs have molecular fractions of $\mathcal{F} \equiv \frac{2N_{\rm H_2}}{2N_{\rm H_2}+N_{\rm H\,I}} \sim 10^{-7}$–0.3 and $V - K \lesssim 4$, whereas the millimetre (and OH) absorbers have molecular fractions $\mathcal{F} \approx 0.6$–1 and optical–near-infrared (optical–near-IR) colours of $V - K \gtrsim 5$ (see fig. 3 of Curran, Whiting & Webb 2010), that is, not only are the radio-band absorbers redder than those of the optical band, but there may also be a correlation between the normalized OH line strength and optical–near-IR colour (Curran et al. 2006), although this requires a larger number of detections for confirmation.

These points strongly suggest that the quasar light is reddened by the dust in the foreground absorber, which prevents the dissociation of the molecules by the ambient UV field. From this it is apparent that in order to detect redshifted molecular absorption with current radio instruments, targets must be selected on the basis of their optical and near-IR photometry, where we select the reddest objects. However, the obscuration responsible for the quasar reddening could be located anywhere between us and the quasar redshift (the three intervening systems are the strongest absorbers, see Section 4.2) and, although wide-band decimetre scans are more efficient than at millimetre wavelengths (Murphy, Curran & Webb 2003; Curran et al. 2005), these are very susceptible to radio frequency interference (RFI). Therefore, in addition to our programme of using the wide-band spectrometer on the Green Bank Telescope (GBT) to perform 200-MHz wide frequency scans of the entire redshift space towards very red, radio-loud objects (see Curran et al. 2007), we are searching for the H I and OH absorption associated with the host galaxy of the quasar. Here we add the results of our recently completed searches for associated absorption and discuss these in the context of our previous search results (Curran et al. 2006, 2008).

## 2 OBSERVATIONS

### 2.1 Sample selection

We observed five sources with the Effelsberg telescope and 11 with the GBT (with two sources, B1107−187 and B1504−166, common to both, Table 1), where the H I 21-cm or OH 18-cm transition fell into an available receiver band. These targets were originally intended to form part of the sample of Curran et al. (2006) and, as such, our targets are largely from the Parkes Half-Jansky Flat-spectrum Sample (PHFS, Drinkwater et al. 1997). These are bright and generally compact radio sources for which there exists comprehensive optical photometry (Francis, Whiting & Webster 2000). From a list of sources, for which the redshifted H I and OH frequencies fell into the available bands, we targeted a specific subsample for each telescope.

(i) For the Effelsberg telescope, our targets were selected on the basis of their having a 'type 2' spectrum, with narrow emission lines, a red continuum and only weak (if any) broad emission-line components. For these, unified schemes of active galactic nuclei (AGNs) imply that our line of sight to the nucleus is blocked by a 'dusty torus' (which obscures the broad-line region and only allows us to view the narrow emission lines directly), through which we may expect to detect absorption. We therefore selected three radio galaxies (B0114+074, B0454+066 and B1555−140[1]) which exhibit optical spectra with narrow emission lines only, indicating the presence of some nuclear extinction. However, as shown by Curran et al. (2008) and Curran & Whiting (2010), the AGN type has little bearing on whether absorption is detected (see Section 4.1).

During the Effelsberg observations (Table 1), due to severe RFI we were encountering at $\lesssim$1.26 GHz, we also selected a lower redshift target, B2352+495 (in which H I 21-cm absorption is detected by Vermeulen et al. 2003), where the OH 18-cm band would be redshifted into the 21-cm band (1345.62 MHz for the $^2\Pi_{3/2} J = 3/2$ $F = 2$–2, 1667-MHz, transition, the transition to which we refer throughout this paper).

(ii) For the GBT, as per Curran et al. (2006), the targets were selected on the basis of their flat radio spectra and very red optical–near-IR colours, properties similar to the (then four, now five) objects with redshifted rotational absorption. Both B0108+388 and B0500+019 have been taken from Carilli et al. (1998) and so are known to exhibit associated H I absorption. The remainder were selected from the PHFS, on the basis of their optical–near-IR photometry (Francis et al. 2000), in which we selected the reddest objects in the sample, the colours of which are believed to be due to dust (Webster et al. 1995).

(iii) In addition to the Effelsberg and GBT targets, we include the unpublished results of searches of other similar sources from Giant Metre-Wave Radio Telescope (GMRT) archival data:

[1] One of the proposed targets, but not observed during this run. We have, however, since detected 21-cm absorption in this with the Australia Telescope Compact Array (ATCA) (Curran et al. 2006).

**Table 1.** The observing details and magnitudes of the targets. $\nu_{exp}$ is the expected frequency (MHz) of the absorption according to the host redshift ($z_{host}$), $t_{obs}$ is the total time on-source (h) and BLs represents the number of baselines used, both after the removal of bad data for the telescope listed. The final columns give the *B*, *V*, *R* and *K* magnitudes.

| Source | $z_{host}$ | Line | $\nu_{exp}$ | Date | $t_{obs}$ | BLs | Telescope | *B* | Reference | *V* | Reference | *R* | Reference | *K* | Reference |
|---|---|---|---|---|---|---|---|---|---|---|---|---|---|---|---|
| COINS J0111+3906 | 0.668 47 | H I | 851 | 7/9/2004 | 2.1 | n/a | GBT | – | – | – | – | 22.0 | S93 | 16.69 | S96 |
| (B0108+388) | ... | OH | 999 | ... | 1.8 | ... | ... | ... | ... | ... | ... | ... | ... | ... | ... |
| [HB89] 0114+074 | 0.342 | H I | 1058 | 9/5/2004 | 0 | n/a | Effelsberg | 20.66 | H01 | – | – | 18.24 | H01 | 15.39 | FPC |
| 4C –00.11 (B0131−001) | 0.879 | H I | 756 | 7–8/2008 | 0.9 | n/a | GBT | 23.3 | F00 | 22.5 | F00 | 20.8 | F00 | 16.8 | F00 |
| ... | ... | OH | 887 | ... | 1.1 | ... | ... | ... | ... | ... | ... | ... | ... | ... | ... |
| 4C –02.09 (B0213−026) | 1.178 | H I | 652 | 31/10/2009 | 1.0 | n/a | GBT | 21.48 | H01 | 20.8 | F00 | 20.48 | H01 | 15.05 | S06 |
| ... | ... | OH | 766 | 17/9/2009 | 1.7 | n/a | GBT | ... | ... | ... | ... | ... | ... | ... | ... |
| 4C –06.21 (B0454+066) | 0.405 | OH | 1187 | 10/5/2004 | 3.7 | n/a | Effelsberg | 19.51 | H01 | – | – | 18.59 | H01 | 15.04 | S06 |
| PKS 0500+019 | 0.584 77 | OH | 1052 | 2/10/2008 | 1.0 | n/a | GBT | 22.5 | D97 | 21.35 | C03 | 20.68 | C03 | 15.43 | FPC |
| B3 0647+415 | 3.797 86 | H I | 296 | 8/2002–2/2003 | 20 | 330–427 | GMRT | – | – | – | – | 21.7 | C90 | 18.6 | C90 |
| ... | ... | OH | 348 | 3/2/2003 | 6.4 | 401 | GMRT | ... | ... | ... | ... | ... | ... | ... | ... |
| B2 0847+37 | 0.406 818 | H I | 1010 | 17/4/2004 | 4.8 | 434 | GMRT | 20.80 | SDR7 | 19.61 | SDR7 | 18.90 | SDR7 | – | – |
| PKS 1107−187 | 0.497 | H I | 949 | 31/1/2009 | 1.7 | n/a | GBT | 22.26 | H01 | 21.1 | F00 | 19.51 | H01 | 15.95 | F00 |
| ... | ... | OH | 1114 | ... | 1.0 | n/a | ... | ... | ... | ... | ... | ... | ... | ... | ... |
| .. | ... | OH | ... | 11/5/2004 | 0 | n/a | Effelsberg | ... | ... | ... | ... | ... | ... | ... | ... |
| TXS 1243+036 | 3.5699 | H I | 311 | 30/8/2003 | 2.3 | 392 | GMRT | 23.08 | SDR7 | 21.56 | SDR7 | 20.67 | SDR7 | – | – |
| ... | ... | OH | 365 | 1/9/2002 | 5.8 | 405 | GMRT | ... | ... | ... | ... | ... | ... | ... | ... |
| PKS 1430−155 | 1.573 | H I | 552 | 15/2/2009 | 0 | n/a | GBT | 22.50 | D97 | 23.2 | F00 | 22.9 | F00 | 17.5 | F00 |
| ... | ... | OH | 648 | ... | 0.1 | n/a | ... | ... | ... | ... | ... | ... | ... | ... | ... |
| [HB89] 1504−166 | 0.876 | H I | 757 | 30/4/2009 | 0.7 | n/a | GBT | 19.05 | D97 | 19.8 | F00 | 19.4 | F00 | 14.0 | F00 |
| ... | ... | OH | 889 | ... | 0 | ... | GBT | ... | ... | ... | ... | ... | ... | ... | ... |
| ... | ... | OH | 889 | 11/5/2004 | 0 | n/a | Effelsberg | ... | ... | ... | ... | ... | ... | ... | ... |
| PKS 1535+004 | 3.497 | H I | 316 | 25/10/2004 | 0 | n/a | GBT | – | – | – | – | – | – | 19.54 | FPC |
| ... | ... | OH | 371 | ... | 1.2 | n/a | GBT | ... | ... | ... | ... | ... | ... | ... | ... |
| B1654−020 | 1.99 | H I | 475 | 6 and 10/10/2008 | 0 | n/a | GBT | 23.70 | D97 | 23.9 | F00 | 23.1 | F00 | 18 | F00 |
| ... | ... | OH | 558 | ... | 1.2 | n/a | ... | ... | ... | ... | ... | ... | ... | ... | ... |
| PKS 1706+006 | 0.449 | H I | 980 | 7/9/2004 | 1.0 | n/a | GBT | 22.00 | H06 | 20.6 | F00 | 20.35 | H06 | 15.6 | F00 |
| ... | ... | OH | 1151 | 30/5/2009 | 1.0 | n/a | GBT | ... | ... | ... | ... | ... | ... | ... | ... |
| PKS 2252−089 | 0.6064 | H I | 884 | 16/7/2009 | 2.0 | n/a | GBT | ... | ... | ... | ... | ... | ... | ... | ... |
| ... | ... | OH | 1038 | 5/6 and 29/9/2009 | 2.0 | n/a | GBT | ... | ... | ... | ... | ... | ... | ... | ... |
| COINS J2355+4950 (B2352+495) | 0.237 83 | OH | 1147 | 12/5/04 | 3.8 | n/a | Effelsberg | 21.10 | H01 | – | – | 18.50 | H01 | 15.11 | S06 |

Photometry references: C90 – Chambers, Miley & van Breugel (1990), O90 – O'Dea, Baum & Morris (1990), S93 – Stanghellini et al. (1993), T93 – Tadhunter et al. (1993), S94 – Stickel & Kühr (1994), S96 – Stickel et al. (1996), D97 – Drinkwater et al. (1997), F00 – Francis et al. (2000), H01 – SuperCOSMOS Sky Survey (Hambly et al. 2001), C03 – Cody & Braun (2003), S06 – 2MASS (Skrutskie et al. 2006), SDR7 – SDSS DR7, A08 – Adelman-McCarthy et al. (2008), and FPC – P. Francis (private communication).

(a) '*Cold gas at high redshift*' (PI: Braun, 02RBa01, 03RBa01), which yielded good data for H I and OH in B0647+415 and B1243+036.

(b) '*H I absorption and emission in radio galaxies at $z \approx 0.4$*' (PI: Blake, 05CBa01), where only one of the five sources searched yielded good data and a detectable flux, B0847+37.

In this paper, we present the results of 14 searches for associated H I absorption and 15 searches for OH. This is in addition to the 7 H I and 14 OH sources searched, using the ATCA and GMRT, by Curran et al. (2006) (with three H I and five OH searches overlapping with this paper), and the 11 H I and seven OH high-redshift ($z \geq 2.9$) sources searched by Curran et al. (2008) (with no overlaps).

### 2.2 Observations

The Effelsberg observations were performed with the 100-m telescope from 2004 May 9 to 12. We used the ultrahigh-frequency (UHF) and 21/18-cm receivers over various bandwidths (in order to cover as wide a redshift range as possible, while minimizing RFI) over 512 channels. Each transition (H I and OH) was observed separately with a requested integration time of 1 h per source per transition (2.25 h with overheads due to position switching and other overheads), which was varied during the observations depending on the severity of the RFI. System temperatures were typically $\lesssim$30 K (when RFI was absent). The data were reduced using the GILDAS and XS packages.

The GBT observations were completed over several sessions in 2004, 2008 and 2009.[2] For all observations, the Prime Focus 1 receiver was used backed by the GBT spectrometer, with a 50-MHz band over 8196 lags giving a channel spacing of 6.104 kHz. Two separate intermediate frequencies (IFs) were employed in order to observe both the H I and the OH lines simultaneously where this was possible and, as per the Effelsberg observations, a total on-time of 1 h per source was requested (a total of 3 h with overheads), although, again, this varied during the actual observations. System temperatures were typically $\approx$20–90 K. The data were reduced using the GBTIDL software, with the the MIRIAD interferometry reduction package being used for the archival GMRT data, with a spectrum extracted from each cube. The observations are summarized in Table 1.

## 3 RESULTS

### 3.1 Observational results

In Fig. 1, we show the final spectra and summarize the values obtained from these in Table 2, where the optical depth limits are quoted per 10 km s$^{-1}$ channel, apart from the low-resolution observation of B2352+495, which is quoted per observed channel. We have detected H I in two (possibly three) of the targets (one of which is a re-detection), Fig. 2, and do not detect OH in any.

### 3.2 H I detections

#### *3.2.1 COINS J0111+3906 (B0108+388)*

In Fig. 2 (left-hand panel), we show the spectrum of the H I 21-cm absorption profile in B0108+388, which was previously detected by Carilli et al. (1998). The fitting of a single Gaussian to the profile gives a peak depth of 18.8 $\pm$ 0.7 mJy (cf. $\approx$73 mJy by Carilli et al. 1998) and a full width at half-maximum (FWHM) of 112 $\pm$ 4 km s$^{-1}$ (cf. 94 $\pm$ 10 km s$^{-1}$) at an observed frequency of 851.326 $\pm$ 0.004 MHz (giving a redshift $z = 0.668\,46$–$0.668\,47$ for the peak of the line). The previous observations were performed with the WSRT, giving a flux density of 180 mJy (cf. our 302 mJy). We use this previously imaged, more resolved, emission to derive an optical depth of $\tau = 0.10$, which, integrated over the FWHM of the profile, gives a column density of $N_{\rm H\,I} = (2.3 \pm 0.2) \times 10^{19} (T_{\rm s}/f)\,{\rm cm}^{-2}$, where $T_{\rm s}$ is the spin temperature of the 21-cm transition and $f$ is the covering factor. This column density is only 30 per cent of the value obtained by Carilli et al. (1998) [$(8.1 \pm 0.2) \times 10^{19} (T_{\rm s}/f)\,{\rm cm}^{-2}$], which we believe is due to their lower quality spectrum.[3]

#### *3.2.2 PKS 1107−187 (B1107−187)*

We also report a possible 21-cm detection in B1107−187. This is apparent in each of the two orthogonal linear polarizations, although with quite different depths – 19.7 $\pm$ 4.5 mJy (at 953.86 $\pm$ 0.01 MHz with FWHM = 34 $\pm$ 9 km s$^{-1}$) in the XX polarization and 9.3 $\pm$ 3.1 mJy (at 953.87 $\pm$ 0.02 MHz with FWHM = 44 $\pm$ 18 km s$^{-1}$) in the YY. The average of the two polarizations, with a single Gaussian fit, gives a line depth of 14.4 $\pm$ 1.8 mJy with a profile width of 50 $\pm$ 11 km s$^{-1}$ (Fig. 2, middle panel), the resulting optical depth of $\tau = 0.016 \pm 0.002$, giving $N_{\rm H\,I} = (1.5 \pm 0.5) \times 10^{18} (T_{\rm s}/f)\,{\rm cm}^{-2}$. The fit is centred on 953.87 $\pm$ 0.01 MHz, giving a redshift of $z = 0.489\,09 \pm 0.000\,02$ (cf. 0.497 quoted in the PHFS, Drinkwater et al. 1997). This suggests that the absorption may be blueshifted by $\approx$1600 km s$^{-1}$ with respect to the galaxy, although the host redshift is known to only three significant figures. Note that of the many features apparent in the OH spectrum (Fig. 1), none gives a $^2\Pi_{3/2}$ $J = 3/2$ $F = 1$–1 (1665 MHz)–$F = 2$–2 (1667 MHz) pair with the same redshift as the 21-cm line.

#### *3.2.3 PKS 2252−090 (B2252−090)*

Finally, we report a new detection of the 21-cm absorption in B2252−090, which was so strong as to be apparent in each 5-min scan. This appears to be composed of two major components (Fig. 2, right-hand panel), one which is narrow and deep ($\tau = 0.129 \pm 0.007$, FWHM = 17 $\pm$ 1 km s$^{-1}$, with $\nu = 883.578 \pm 0.001$ MHz giving $z = 0.607\,56$) and the other shallow, wide blueshifted tail ($\tau = 0.076 \pm 0.003$, FWHM = 94 $\pm$ 5 km s$^{-1}$, with $\nu = 883.664 \pm 0.008$ MHz giving $z = 0.607\,41 \pm 0.000\,02$). A single Gaussian fit to the absorption gives $\tau = 0.12 \pm 0.01$ and FWHM = 85 $\pm$ 10 km s$^{-1}$ (centred on $\nu = 883.62 \pm 0.01$ MHz $\Rightarrow z = 0.607\,48 \pm 0.000\,02$), with the velocity-integrated optical depth giving $N_{\rm H\,I} = 2.0 \pm 0.4 \times 10^{19} (T_{\rm s}/f)\,{\rm cm}^{-2}$. This, along with B0108+338, is close to the maximum line strength detected in redshifted 21-cm absorption.

[2] Originally intended to be completed in 2004, thus being added to the sample of Curran et al. (2006) (Section 2.1).

[3] $N_{\rm H\,I} = (8.1 \pm 0.2) \times 10^{19} (T_{\rm s}/f)\,{\rm cm}^{-2}$ is the value derived using a Gaussian fit, whereas summing the actual channels over which the absorption occurs gives $(8.0 \pm 2.2) \times 10^{19}$ $(T_{\rm s}/f)\,{\rm cm}^{-2}$. Applying this summing to our profile gives $(2.2 \pm 0.2) \times 10^{19}$ $(T_{\rm s}/f)\,{\rm cm}^{-2}$, that is, the same as the Gaussian fit.

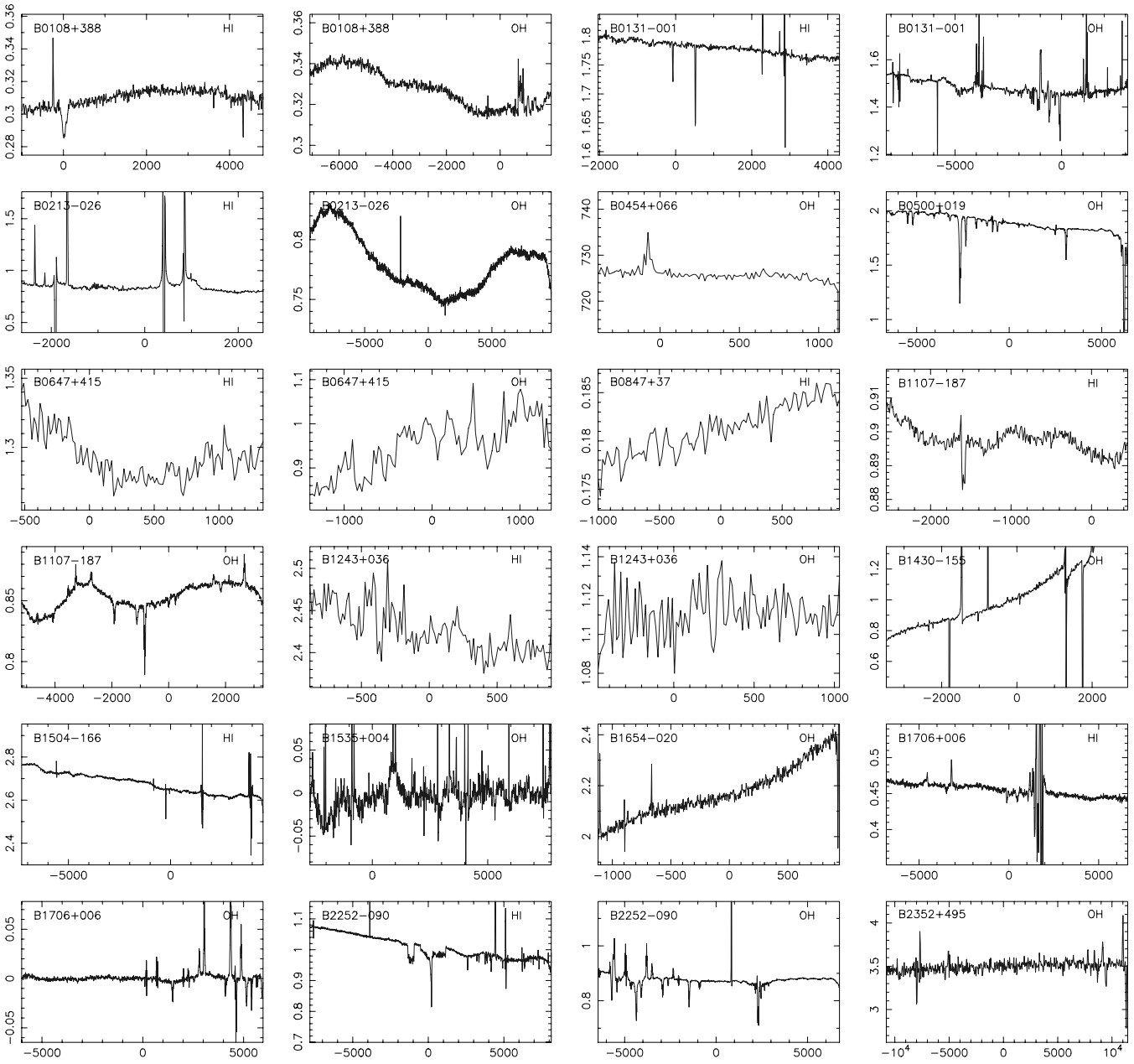


**Figure 1.** The useable spectra before baseline removal. The abscissa is in km s$^{-1}$ with respect to the optical redshift and for the GBT and GMRT spectra, the ordinate shows the flux density (Jy), whereas for the Effelsberg spectra (B0454+066 and B2352+495), this is in antenna temperature, $T_{\rm A}^{*}$ (K) (the sensitivity is 1.55 K Jy$^{-1}$ in the UHF band and 1.50 K Jy$^{-1}$ in the 21/18-cm band). The Effelsberg and GBT spectra are shown at a resolution of 10 km s$^{-1}$ (except for B1654−020 which is shown at the observed 3.3 km s$^{-1}$ and B2352+495 at the observed 43.5 km s$^{-1}$) and the GMRT spectra are shown at their observed channel spacings (>10 km s$^{-1}$, see Table 2). Since the spectra exhibited negative flux densities, the B1535+004 and B1706+006 OH spectra after baseline removal are shown. Note that we believe the features close to 0 km s$^{-1}$ in the B1706+006 H I spectrum are due to RFI and that the flux density for B0847+37, which is resolved in the GMRT image, is over the central beam only.

## 4 DISCUSSION

### 4.1 H I results

For the 21-cm searches, we have obtained one, possibly two new detections, confirming and improving upon a previous detection. From Fig. 3, we see a range of 1216 Å luminosities (listed in Table 2): Curran et al. (2008) found a critical luminosity ($L_{\rm UV} \sim 10^{23}$ W Hz$^{-1}$) at this wavelength, above which 21-cm absorption has never been detected. All but two of the sample lie below this threshold, these being B0647+415 and B1243+036 (Table 2), which, as our previous $z \sim 3$–4 searches (Curran et al. 2008), are above the critical luminosity due to their high redshifts, causing the selection of the brightest sources, despite their relatively faint magnitudes (Table 1, cf. fig. 5 of Curran et al. 2010). These two new high-redshift sources differ from all of the other $L_{\rm UV} \gtrsim 10^{23}$ W Hz$^{-1}$ targets searched in 21-cm detection in that they are type 2 objects. Their inclusion increases the significance of the UV luminosity effect, with the

**Table 2.** The observational results. $\nu_{\rm obs}$ is the observed frequency range of the line over which the quoted rms level is applicable, $\sigma_{\rm rms}$ is the rms noise reached per $\Delta v$ channel after subtraction of a low-order baseline, $S_{\rm cont}$ is the continuum flux density, $\tau$ is the optical depth of the line, where $\tau = -\ln(1-3\sigma_{\rm rms}/S_{\rm cont})$ is quoted for the non-detections, calculated for a 10 km s$^{-1}$ channel (except for B2352+495, see main text). These give the quoted column densities, where $T_{\rm s}$ is the spin temperature of the H I 21-cm absorption, $T_{\rm x}$ is the excitation temperature (K) of the OH and $f$ is the respective covering factor. The final columns give the AGN type and 1216 Å luminosity (W Hz$^{-1}$), determined/calculated as per Curran et al. (2008).

| Source | Line | $\nu_{\rm obs}$ (MHz) | $\sigma_{\rm rms}$ (mJy) | $\Delta v$ (km s$^{-1}$) | $S_{\rm cont}$ (Jy) | $\tau$ | $N$ (cm$^{-2}$) | Class | Type | Reference | log $L_{\rm UV}$ |
|---|---|---|---|---|---|---|---|---|---|---|---|
| B0108+388 | H I | 837.6–854.9 | 1.0[a] | 2.15 | 0.303 | 0.10 | $(2.3 \pm 0.2) \times 10^{19}$ $(T_{\rm s}/f)$ | Gal | 2 | L96 | 20.309 |
| ... | OH | 996.8–1023.0 | 3.6[b] | 1.83 | 0.314 | <0.015 | $<3.6 \times 10^{13}$ $(T_{\rm x}/f)$ | ... | ... | ... | ... |
| B0131−001 | H I | 753.7–757.6 | 3.7 | 2.42 | 1.76 | <0.0031 | $<5.7 \times 10^{16}$ $(T_{\rm s}/f)$ | QSO | – | – | 20.221 |
| ... | OH | 885.8–888.0 | 5.1 | 2.06 | 1.51 | <0.0046 | $<1.1 \times 10^{13}$ $(T_{\rm x}/f)$ | ... | ... | ... | ... |
| B0213−026 | H I | 651.4–655.7 | 243 | 0.35 | 0.913 | <0.16 | $<2.9 \times 10^{18}$ $(T_{\rm s}/f)$ | QSO | 2 | D97a | 22.119 |
| ... | OH | 742.6–786.6 | 5.2 | 2.40 | 0.756 | <0.010 | $<2.4 \times 10^{13}$ $(T_{\rm x}/f)$ | ... | ... | ... | ... |
| B0454+066 | OH | 1182.2–1188.4 | 45 | 3.09 | 0.55[c] | <0.15 | $<3.6 \times 10^{14}$ $(T_{\rm x}/f)$ | QSO | 2 | D97a | 21.567 |
| B0500+019 | OH | 1050.4–1052.5 | 11[d] | 0.87 | 1.89 | <0.0052 | $<1.2 \times 10^{13}$ $(T_{\rm x}/f)$ | Gal | 2 | H03 | 20.367 |
| B0647+415 | H I | 295.1–296.9 | 17 | 15.8 | 1.29 | <0.050 | $<9.1 \times 10^{17}$ $(T_{\rm s}/f)$ | Gal | 2 | D97b | 23.258 |
| ... | OH | 346.4–349.6 | 63 | 26.9 | 0.949 | <0.40 | $<9.5 \times 10^{14}$ $(T_{\rm x}/f)$ | ... | ... | ... | ... |
| B0847+37 | H I | 1005.8–1013.3 | 1.7 | 18.6 | 187 | <0.037 | $<6.8 \times 10^{17}$ $(T_{\rm s}/f)$ | Gal | 2 | SDR7 | 20.930 |
| B1107−187 | H I | 947.6–957.3 | 4.1 | 1.93 | 0.896 | 0.016[e] | $(1.5 \pm 0.5) \times 10^{18}$ $(T_{\rm s}/f)$* | Gal | 1 | D97a | 19.157 |
| ... | OH | 1101.5–1133.2 | 5.4 | 1.65 | 0.853 | <0.0077 | $<1.8 \times 10^{13}$ $(T_{\rm x}/f)$ | ... | ... | ... | .. |
| B1243+036 | H I | 309.9–311.7 | 28 | 15.1 | 2.43 | <0.042 | $<7.7 \times 10^{17}$ $(T_{\rm s}/f)$ | Gal | 2 | R97 | 23.382 |
| ... | OH | 363.6–365.4 | 12 | 12.8 | 1.11 | <0.037 | $<8.8 \times 10^{13}$ $(T_{\rm x}/f)$ | ... | ... | ... | ... |
| B1430−155 | OH | 645.4–649.6 | 24 | 2.83 | 1.03 | <0.037 | $<8.8 \times 10^{13}$ $(T_{\rm x}/f)$ | QSO | 1 | D97a | 21.790 |
| B1504−166 | H I | 754.1–774.6 | 52 | 2.42 | 2.62 | <0.012 | $<2.2 \times 10^{17}$ $(T_{\rm s}/f)$ | QSO | 1 | H78 | 22.361 |
| B1535+004 | OH | 369.6–371.8 | 15[g] | 4.94 | – | <0.08 | $<1.9 \times 10^{14}$ $(T_{\rm x}/f)$ | QSO | – | – | – |
| B1654−020 | OH | 556.1–559.7 | 18 | 3.28 | 2.20 | <0.014 | $<3.3 \times 10^{13}$ $(T_{\rm x}/f)$ | Gal | 1 | D97a | 22.151 |
| B1706+006 | H I | 960.4–990.3[h] | 5.2 | 1.87 | 0.453 | <0.015 | $<2.7 \times 10^{17}$ $(T_{\rm s}/f)$ | Gal | 2 | D97a | 19.838 |
| ... | OH | 1140.3–1171.0 | 5.4 | 1.59 | 0.524[i] | <0.0010 | $<2.5 \times 10^{13}$ $(T_{\rm x}/f)$ | ... | ... | ... | ... |
| B2252−090 | H I | 873.8–908.1 | 1.0 | 5.6[j] | 0.990 | 0.11 | $(2.0 \pm 0.4) \times 10^{19}$ $(T_{\rm s}/f)$ | Gal | 2 | D97a | 20.802 |
| ... | OH | 1031.6–1040.5 | 2.9 | 1.77 | 0.871 | <0.0042 | $<1.0 \times 10^{13}$ $(T_{\rm x}/f)$ | ... | ... | ... | ... |
| B2352+495 | OH | 1313.7–1380.4 | 32[k] | 43.5 | 2.25 | <0.043 | $<1.0 \times 10^{13}$ $(T_{\rm x}/f)$ | Gal | 2 | L96 | 19.030 |

References: H78 – Hunstead, Murdoch & Shobbrook (1978), L96 – Lawrence et al. (1996), D97a – Drinkwater et al. (1997), D97b – Dey et al. (1997), R97 – Roettgering et al. (1997), H03 – Hook et al. (2003) and SDR7 – SDSS DR7.

Notes. [a]Detected previously by Carilli et al. (1998) (Section 3.2.1); [b]also undetected at an rms of 2.9 mJy per 19 km s$^{-1}$ channel with the GMRT (Curran et al. 2006); [c]as the flux density of the source could not be determined, this is derived using the a flux density of 0.55 Jy, estimated from the neighbouring 408- and 1400-MHz values (Douglas et al. 1996; Condon et al. 1998); [d]H I detected by Carilli et al. (1998), OH previously undetected at an rms of 7.4 mJy per 18 km s$^{-1}$ channel with the GMRT (Curran et al. 2006); [e]$\tau < 0.0060$ if detection is not real (Section 3.2.2); [f]OH previously undetected at an rms of 2.4 mJy per 17 km s$^{-1}$ channel with the GMRT (Curran et al. 2006); [g]H I undetected at an rms of 7.3 mJy per 15 km s$^{-1}$ channel with the GMRT (Curran et al. 2006) and the optical depth calculated using $S_{365\,\rm MHz} = 0.389$ Jy (Douglas et al. 1996); [h]neglecting the RFI at 973.5–977.6 MHz; [i]from the 2004 observations; [j]15 mJy in the vicinity of the absorption feature (880.79–888.34 MHz); and [k]H I detected by Vermeulen et al. (2003). *$N_{\rm H\,I} < 1.1 \times 10^{17}(T_{\rm s}/f)$ cm$^{-2}$ at $z = 0.483\,81$–$0.498\,98$ over the absorption-free region in case of a false detection.

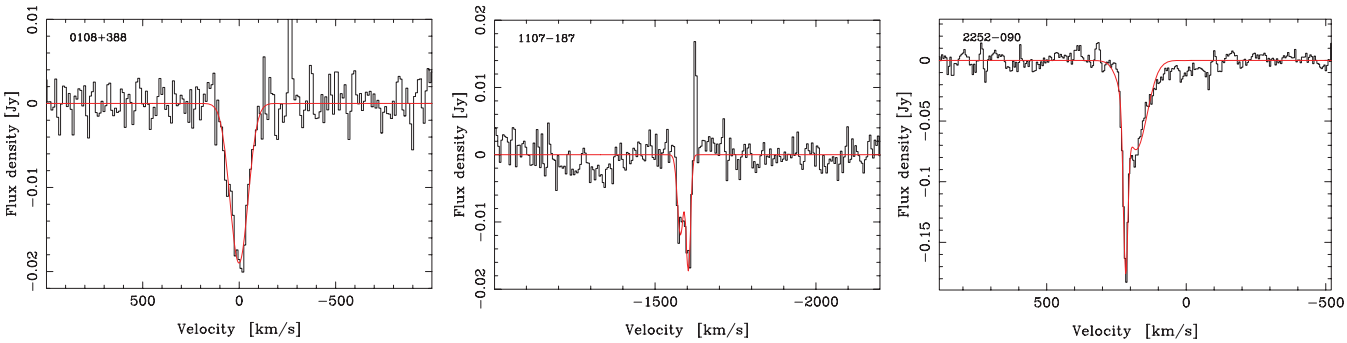


**Figure 2.** Left-hand panel: single Gaussian fit to the H I absorption in B0108+388 shown at a resolution of 10 km s$^{-1}$. The velocity scale is relative to 851.32 MHz. Middle panel: two Gaussian fit to the possible H I absorption towards B1107−187 shown at a resolution of 5 km s$^{-1}$. The velocity scale is relative to 948.83 MHz and the fits give a 17-mJy-deep feature at $z = 0.489\,05$ with a FWHM = 16 km s$^{-1}$ and a 12-mJy-deep feature at $z = 0.489\,17$ with a FWHM = 22 km s$^{-1}$. Right-hand panel: two Gaussian fits to the H I absorption in B2252−090 shown at a resolution of 5 km s$^{-1}$. The velocity scale is relative to 884.22 MHz.

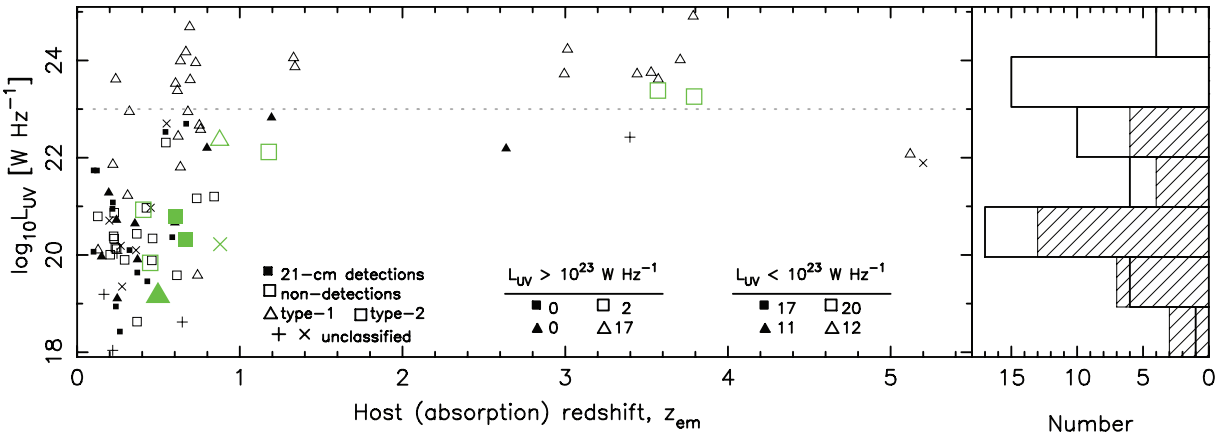


**Figure 3.** The UV ($\lambda \approx 1216$ Å) luminosity versus the host redshift for the $z \geq 0.1$ radio galaxies and quasars searched in associated 21-cm absorption. The filled symbols/hatched histograms represent the 21-cm detections and the unfilled symbols/unfilled histograms represent the non-detections, with the large coloured symbols designating the new results presented here (B1107−187 is treated as a detection, Section 3.2.2). The shapes represent the AGN classifications, with triangles representing type 1 objects and squares type 2 objects. The symbols + and × designate an undetermined AGN type for a detection and non-detection, respectively. The legend shows the number of each AGN type according to the $L_{\rm UV} = 10^{23}$ W Hz$^{-1}$ partition.

binomial probability of zero out of 19 detections occurring by chance being just $1.9 \times 10^{-6}$, if a 21-cm detection and non-detection are equally probable. Assuming Gaussian statistics, this corresponds to a significance of $4.76\sigma$.

As mentioned in Section 2.1, the distribution of 21-cm detections in radio galaxies and quasars is usually attributed to unified schemes of AGNs (Antonucci 1993; Urry & Padovani 1995), where, due to the edge-on torus of the dense circumnuclear material, type 2 objects (usually galaxies) present a thick column of the intervening gas along our sight-line and thus absorb in 21-cm detections (Jaffe & McNamara 1994; Conway & Blanco 1995), whereas type 1 objects (usually quasars) do not. Of the new detections, one is type 2 and the other is type 1 (assuming that B1107−187 is a detection, Section 3.2.2), contributing to a type 2 detection rate of 46 per cent and a type 1 detection rate of 48 per cent; these confirm our previous finding that unified schemes of AGNs cannot be used to explain the incidence of the 21-cm absorption in these objects (cf. Morganti et al. 2001; Pihlström, Conway & Vermeulen 2003; Gupta et al. 2006; Gupta & Saikia 2006). That is, these results further support our suggestion that the bulk of the cool gas is located in the main galactic disc, which is randomly oriented with respect to the torus of the obscuring material invoked by unified schemes of AGNs (Curran & Whiting 2010).

### 4.2 OH results

Although OH was not detected in any of the sample from the H I detections,[4] we can obtain normalized OH line strength limits in order to compare with the five detected OH absorbers. In Fig. 4, we add the new results to the molecular line strength–optical–near-IR colour correlation found by Curran et al. (2006), showing also the corresponding distributions using the blue and red magnitudes. Since the FWHM of the OH lines are expected to be close to those of the 21-cm profiles (Curran et al. 2007), as per Curran et al. (2008), we have rescaled the OH column density limits by $\sqrt{\rm FWHM_{H\,I}/\Delta v}$, in order to give the limit of a single channel 'smoothed' to $\rm FWHM_{OH} \approx FWHM_{H\,I}$. This should give a more accurate estimate of the upper limit than quoting this per $\Delta v$ channel.[5]

[4] B0108+388, B0500+019, B1107−187, B2352+495 (this paper), B0902+343 (Cody & Braun 2003), J1124+1919, J1347+1217 and J2316+0404 (Gupta et al. 2006).

[5] $\Delta v$ is the original resolution of the observations or 10 km s$^{-1}$ used in Table 1 and $\rm FWHM_{H\,I}$ is obtained from Mirabel (1989), Carilli et al. (1998), Cody & Braun (2003), Vermeulen et al. (2003) and Gupta et al. (2006), as well as this paper (Section 3.2).

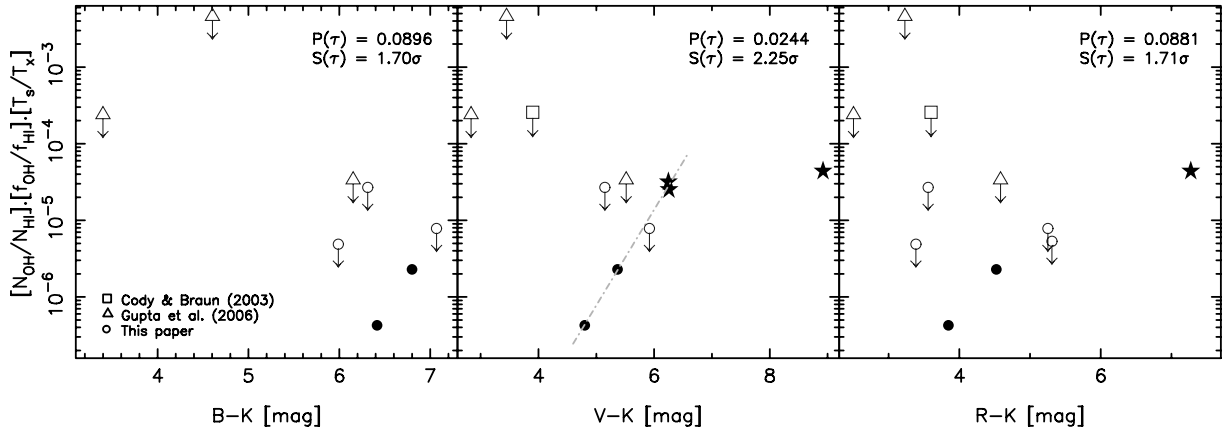


**Figure 4.** The normalized OH $^2\Pi_{3/2}J = 3/2$ (1667-MHz) line strength ($2.38 \times 10^{14} \int \tau_{\rm OH}\,{\rm d}v / 1.82 \times 10^{18} \int \tau_{\rm H\,I}\,{\rm d}v$) versus the blue–near-IR (left-hand panel), optical–near-IR (middle panel) and red–near-IR (right-hand panel) colour. The filled symbols show the five known OH absorbers (the stars designate intervening absorbers, see Curran et al. 2006 and references therein) and the unfilled symbols represent the H I 21-cm detections with OH upper limits. The probability of each distribution occurring by chance is shown, along with the associated significance (see main text). The line shows the least-squares fit to those also detected in millimetre-band molecular transitions for the optical–near-IR colours (Curran et al. 2006).

From this, we see that, even if the reddening of the quasar light does occur within its host galaxy and not at some intervening redshift, according to the five known OH absorbers, only B0500+019 and (from the $R-K$ plot) B0108+388 may have been searched sufficiently deeply. Although the limit is close to the expected detection threshold, B0500+019 is also undetected in $HCO^+$, to limits which are significantly stronger according to the $N_{\rm HCO+} - V - K$ correlation (Curran et al., in preparation), and so perhaps the reddening of this source does not occur in the host galaxy but is the cause of some intervening absorbers.[6]

Note finally that the addition of these limits through the ASURV survival analysis package (Isobe, Feigelson & Nelson 1986) increases the significance of the $V-K$ correlation over that for the OH detections only [$S(\tau) = 1.96\sigma$, Curran et al. 2006]. For the $B-K$ and $R-K$ correlations, the significance is somewhat lower, although, due to the limited availability of these magnitudes for the known absorbers, this is not surprising being based upon only two or three detections.

## 5 SUMMARY

We have undertaken a survey for the redshifted H I 21-cm and OH 18-cm absorption in a sample of type 2 AGNs and reddened flat spectrum objects with the Effelsberg telescope and GBT. We also include unpublished searches of similar objects with the GMRT. Of the 10 objects for which there are useful data, we report one new clear 21-cm detection, in addition to a possible detection, and confirm and significantly improve upon a previous detection (all with the GBT). The selection criteria for the targets pre-date the findings of Curran et al. (2008), although they confirm these.

(i) All of the 21-cm detections occur in objects with $\lambda = 1216$ Å luminosities of $L_{\rm UV} \leq 10^{23}$ W Hz$^{-1}$, a range within which there are also four new non-detections. All of the detections arise in galaxies (as opposed to quasars), which have been noted to have higher 21-cm detection rates (52 per cent for galaxies compared to 17 per cent for quasars), this being attributed to galaxies tending to be type 2 objects. However, Curran & Whiting (2010) have shown that the higher detection rate in galaxies is likely to be a consequence of their generally lower UV luminosities, as opposed to their AGN classification.

(ii) The two objects for which $L_{\rm UV} > 10^{23}$ W Hz$^{-1}$ remain undetected, confirming that the UV luminosity is an important criterion in the detection of cool neutral gas (Curran & Whiting 2010). Their inclusion, the first published type 2 $L_{\rm UV} > 10^{23}$ W Hz$^{-1}$ sources searched for in 21-cm detection, raises the significance of the UV luminosity–21-cm anticorrelation to $4.76\sigma$.

(iii) At $L_{\rm UV} \leq 10^{23}$ W Hz$^{-1}$, the detection rates for both type 1 and type 2 objects remain close to 50 per cent, supporting the hypothesis that unified schemes of AGNs cannot account for the observed incidence of the 21-cm absorption in radio galaxies and quasars.

14 of the sources searched in OH had useful data, although only two of these have 21-cm detections, thus being able to yield limits on the normalized line strengths. Adding those from the literature gives a total of eight objects for which we can normalize the line strengths and thus compare with the five known OH absorbers. On this basis, however, we find that only two (B0108+388 and B0500+019, both from this paper) come close to having been searched deeply enough. This confirms the findings of Curran et al. (2006) that many of the known objects are simply not 'red enough' to indicate sufficiently large columns of dust, conducive to the presence of molecular gas, along their sight-lines.

## ACKNOWLEDGMENTS

We would like to thank the anonymous referee for their helpful comments, Christian Henkel for the information on the Effelsberg telescope, Chris Blake for his GMRT data (05CBa01), and Kamble Jayprakash and Yogesh Wadadekar for their assistance in accessing the archival GMRT data (02RBa01 and 03RBa01, respectively). Also, many thanks to Cormac 'Mopra Boy' Purcell for his fabulous SDFITS2FITS script, which allowed easy manipulation of the reduced GBT data, and Anant Tanna for the digitized spectrum of 0108+388 from Carilli et al. (1998). MTM thanks the STFC for

[6] <30 per cent of the redshift space towards B0500+019 has been scanned for $HCO^+$ (Murphy et al. 2003), although the detection of OH does not ensure the detection of a millimetre transition (Kanekar et al. 2005).

an Advanced Fellowship and the Australian Research Council for a QEII Research Fellowship (DP0877998).

This research has made use of the NASA/IPAC Extragalactic Data base which is operated by the Jet Propulsion Laboratory, California Institute of Technology, under contract with the National Aeronautics and Space Administration (NASA). This research has also made use of the NASA's Astrophysics Data System Bibliographic Services and ASURV Rev 1.2 (Lavalley, Isobe & Feigelson 1992), which implements the methods presented in Isobe et al. (1986).

The Two-Micron All-Sky Survey is a joint project of the University of Massachusetts and the Infrared Processing and Analysis Center/California Institute of Technology funded by the NASA and the National Science Foundation.

## REFERENCES

Adelman-McCarthy J. K., Agüeros M. A., Allam S. S., Anderson K. S. J., Anderson S. F., Annis J., Bahcall N. A., Baldry I. K., 2008, ApJS, 175, 297
Antonucci R. R. J., 1993, ARA&A, 31, 473
Carilli C. L., Menten K. M., Reid M. J., Rupen M. P., Yun M. S., 1998, ApJ, 494, 175
Carilli C. L., Gnedin N., Furlanetto S., Owen F., 2004, New Astron. Rev., 48, 1053
Chambers K. C., Miley G. K., van Breugel W. J. M., 1990, ApJ, 363, 21
Chengalur J. N., de Bruyn A. G., Narasimha D., 1999, A&A, 343, L79
Cody A. M., Braun R., 2003, A&A, 400, 871
Condon J. J., Cotton W. D., Greisen E. W., Yin Q. F., Perley R. A., Taylor G. B., Broderick J. J., 1998, AJ, 115, 1693
Conway J. E., Blanco P. R., 1995, ApJ, 449, L131
Curran S. J., 2010, MNRAS, 402, 2657
Curran S. J., Whiting M. T., 2010, ApJ, 712, 303
Curran S. J., Kanekar N., Darling J. K., 2004a, New Astron. Rev., 48, 1095
Curran S. J., Murphy M. T., Pihlström Y. M., Webb J. K., Bolatto A. D., Bower G. C., 2004b, MNRAS, 352, 563
Curran S. J., Webb J. K., Murphy M. T., Kuno N., 2005, in Engvold O., ed., ASP Conf. Ser. Vol. 13, Highlights of Astronomy. Astron. Soc. Pac., San Francisco, p. 845
Curran S. J., Whiting M., Murphy M. T., Webb J. K., Longmore S. N., Pihlström Y. M., Athreya R., Blake C., 2006, MNRAS, 371, 431
Curran S. J., Darling J. K., Bolatto A. D., Whiting M. T., Bignell C., Webb J. K., 2007, MNRAS, 382, L11
Curran S. J., Whiting M. T., Wiklind T., Webb J. K., Murphy M. T., Purcell C. R., 2008, MNRAS, 391, 765
Curran S. J., Whiting M. T., Webb J. K., 2010, in Heald G., Serra P., eds, Proc. Sci., Vol. 89, Panoramic Radio Astronomy. SISSA, Trieste, http://pos.sissa.it/
Darling J., 2003, Phys. Rev. Lett., 91, 011301
Dey A., van Breugel W., Vacca W. D., Antonucci R., 1997, ApJ, 490, 698
Douglas J. N., Bash F. N., Bozyan F. A., Torrence G. W., Wolfe C., 1996, AJ, 111, 1945
Drinkwater M. J. et al., 1997, MNRAS, 284, 85
Francis P. J., Whiting M. T., Webster R. L., 2000, PASA, 17, 56
Gupta N., Saikia D. J., 2006, MNRAS, 370, 738
Gupta N., Salter C. J., Saikia D. J., Ghosh T., Jeyakumar S., 2006, MNRAS, 373, 972
Hambly N. et al., 2001, MNRAS, 326, 1279
Hook I. M., Shaver P. A., Jackson C. A., Wall J. V., Kellermann K. I., 2003, A&A, 399, 469
Hunstead R. W., Murdoch H. S., Shobbrook R. R., 1978, MNRAS, 185, 149
Isobe T., Feigelson E., Nelson P., 1986, ApJ, 306, 490
Jaffe W., McNamara B. R., 1994, ApJ, 434, 110
Jorgenson R. A., Wolfe A. M., Prochaska J. X., Carswell R. F., 2009, ApJ, 704, 247
Kanekar N., Chengalur J. N., 2002, A&A, 381, L73
Kanekar N., Chengalur J. N., de Bruyn A. G., Narasimha D., 2003, MNRAS, 345, L7
Kanekar N. et al., 2005, Phys. Rev. Lett., 95, 261301
Kanekar N., Prochaska J. X., Ellison S. L., Chengalur J. N., 2009, MNRAS, 396, 385
Lavalley M. P., Isobe T., Feigelson E. D., 1992, BAAS, 24, 839
Lawrence C. R., Zucker J. R., Readhead A. C. S., Unwin S. C., Pearson T. J., Xu W., 1996, ApJS, 107, 541
Mirabel I. F., 1989, ApJ, 340, L13
Morganti R., Oosterloo T. A., Tadhunter C. N., van Moorsel G., Killeen N., Wills K. A., 2001, MNRAS, 323, 331
Murphy M. T., Curran S. J., Webb J. K., 2003, MNRAS, 342, 830
Noterdaeme P., Ledoux C., Petitjean P., Srianand R., 2008, A&A, 481, 327
O'Dea C. P., Baum S. A., Morris G. B., 1990, A&AS, 82, 261
Pihlström Y. M., Conway J. E., Vermeulen R. C., 2003, A&A, 404, 871
Roettgering H. J. A., van Ojik R., Miley G. K., Chambers K. C., van Breugel W. J. M., de Koff S., 1997, A&A, 326, 505
Skrutskie M. F., Cutri R. M., Stiening R., Weinberg M. D., Schneider S., Carpenter J. M., Beichman C., Capps R. M., 2006, AJ, 131, 1163
Srianand R., Gupta N., Petitjean P., Noterdaeme P., Ledoux C., 2010, MNRAS, p. 1888
Stanghellini C., O'Dea C. P., Baum S. A., Laurikainen E., 1993, ApJS, 88, 1
Stickel M., Kühr H., 1994, A&AS, 105, 67
Stickel M., Rieke G. H., Kühr H., Rieke M. J., 1996, ApJ, 468, 556
Tadhunter C. N., Morganti R., di Serego-Alighieri S., Fosbury R. A. E., Danziger I. J., 1993, MNRAS, 263, 999
Tzanavaris P., Murphy M. T., Webb J. K., Flambaum V. V., Curran S. J., 2007, MNRAS, 374, 634
Urry C. M., Padovani P., 1995, PASP, 107, 803
Vermeulen R. C. et al., 2003, A&A, 404, 861
Webster R. L., Francis P. J., Peterson B. A., Drinkwater M. J., Masci F. J., 1995, Nat, 375, 469

This paper has been typeset from a TEX/LATEX file prepared by the author.